

## Research Article

# Calcium Dyshomeostasis Alters CCL5 Signaling in Differentiated PC12 Cells

Tomasz Radzik,<sup>1</sup> Tomasz Boczek ,<sup>1,2</sup> Bożena Ferenc,<sup>1</sup> Maciej Studzian,<sup>3</sup> Lukasz Pulaski,<sup>3,4</sup> and Ludmila Zylinska <sup>1</sup>

<sup>1</sup>Department of Molecular Neurochemistry, Medical University, 6/8 Mazowiecka Str., 92-215 Lodz, Poland

<sup>2</sup>Department of Ophthalmology, Stanford University School of Medicine, 1651 Page Mill Road, Palo Alto, 94304, USA

<sup>3</sup>Department of Molecular Biophysics, University of Lodz, 12/16 Banacha Str., 90-237 Lodz, Poland

<sup>4</sup>Laboratory of Transcriptional Regulation, Institute of Medical Biology PAS, 106 Lodowa Str., 93-232 Lodz, Poland

Correspondence should be addressed to Ludmila Zylinska; ludmila.zylinska@umed.lodz.pl

Received 11 January 2019; Accepted 4 March 2019; Published 26 March 2019

Guest Editor: Hailong An

Copyright © 2019 Tomasz Radzik et al. This is an open access article distributed under the Creative Commons Attribution License, which permits unrestricted use, distribution, and reproduction in any medium, provided the original work is properly cited.

**Background.** Plasma membrane  $\text{Ca}^{2+}$ -ATPase (PMCA) is the most sensitive cellular calcium detector. It exists in four main isoforms (PMCA1-4), among which PMCA2 and PMCA3 are considered as fast-acting neuron-specific forms. In the brain, PMCA function declines progressively during aging; thereby impaired calcium homeostasis may contribute to some neurodegenerative diseases. These destructive processes can be propagated by proinflammatory chemokines, including chemokine CCL5, which causes phospholipase C-mediated liberation of  $\text{Ca}^{2+}$  from endoplasmic reticulum by  $\text{IP}_3$ -gated channels. **Methods.** To mimic the changes in aged neurons we used stable transfected differentiated PC12 cells with downregulated PMCA2 or PMCA3 and analyzed the effect of CCL5 on calcium transients with Fluo-4 reagent. Chemokine receptors were evaluated using Western blot, and  $\text{IP}_3$  receptors expression level was assessed using qRT-PCR and Western blot. **Results.** In PMCA-reduced cell lines, CCL5 released more  $\text{Ca}^{2+}$  by  $\text{IP}_3$ -sensitive receptors, and the time required for  $\text{Ca}^{2+}$  clearance was significantly longer. Also, in these lines we detected altered expression level of CCR5 and  $\text{IP}_3$  receptors. **Conclusion.** Although modification of PMCA composition could provide some protection against calcium overload, reduction of PMCA2 appeared to be more detrimental to the cells than deficiency of PMCA3. Under pathological conditions, including inflammatory CCL5 action and long-lasting  $\text{Ca}^{2+}$  dyshomeostasis, insufficient cell protection may result in progressive degeneration and death of neurons.

## 1. Introduction

Growing body of evidence suggests that disrupted calcium homeostasis plays a detrimental role in triggering neurodegeneration. This process can also be propagated by repeated inflammatory reactions, including local production of chemokines. These events intensify particularly during aging, when the proper response to extracellular signals is decreased due to accumulation of multiple cellular damage and pathologies [1–4]. Injured cells are exposed to a prolonged elevation of intracellular  $\text{Ca}^{2+}$  that in turn initiates a number of abnormal processes, which can finally lead to cell death [5–7]. Disturbances in calcium homeostasis have been attributed to imbalance between calcium “on” and “off” systems, which affects cell survival. In healthy cells, the first

step in decreasing cytosolic  $\text{Ca}^{2+}$  relies on three modes: uptake into endoplasmic reticulum by sarco/endoplasmic  $\text{Ca}^{2+}$ -ATPase (SERCA), extrusion by high-capacity but low-affinity  $\text{Na}^+/\text{Ca}^{2+}$  exchanger (NCX), and removal by plasma membrane  $\text{Ca}^{2+}$ -ATPase (PMCA) [8, 9]. The latter is the most sensitive element with low capacity, but very high affinity. The enzyme is represented by 4 main isoforms with ~30 variants that exhibit differential spatial and developmental expression pattern [10, 11]. The two ubiquitous isoforms, PMCA1 and PMCA4, are far less effective in controlling calcium homeostasis than the two neuron-specific PMCA2 and PMCA3 isoforms. The expression profile of PMCA changes significantly during development, reflecting the specific function of each isoform. Changes in PMCA expression and activity have also been reported during aging. It is believed that PMCA

loss may significantly impair calcium extrusion in senescence neurons making them more susceptible to neurotoxic insults [12–17].  $\text{Ca}^{2+}$ -mediated neurotoxicity has been shown for several neurodegenerative diseases including Alzheimer's disease (AD), Huntington disease (HD), spinocerebellar ataxias (SCAs), Parkinson's disease (PD), schizophrenia, or bipolar disorder [6, 15, 18–22].

Additional factors contributing to neuronal death are inflammatory mediators, including some chemokines [1, 23]. Among 50 discovered chemokines, chemokine C-C motif ligand 5 (CCL5, RANTES) is of particular interest due to its potential role as a modulator of cellular metabolism and brain architecture [23–25]. CCL5 is constitutively expressed in the adult central nervous system, with region-specific expression pattern [26]. A remarkable increase of CCL5 in central nervous system (CNS) can be detected during permeabilization of the blood–brain barrier and after extensive production of CCL5 from astrocytes and microglial cells, triggered by proinflammatory factors [27–31]. One of the mechanisms of action of CCL5 is a positive control of cytosolic  $\text{Ca}^{2+}$  mobilization after binding to three receptors: CCRI, CCR3, and CCR5 [23, 32]. They are cell surface-associated, immune-regulatory G protein-coupled receptors (GPCRs). CCL5 binding activates a G protein, which subsequently activates phospholipase C (PLC) involved in a second messenger system. PLC-mediated hydrolysis of phosphatidylinositol 4,5-bisphosphate ( $\text{PIP}_2$ ) gives rise to two products: 1,2-diacylglycerol and inositol 1,4,5-triphosphate ( $\text{IP}_3$ ).  $\text{IP}_3$  stimulates the release of  $\text{Ca}^{2+}$  from intracellular stores through  $\text{IP}_3$  receptors, which exist in three different isoforms [33–35].

The present study was undertaken to clarify the potential role of CCL5-mediated signaling using the model of differentiated PC12 cells, which is one of the most frequently used models for studying neuronal processes. We have previously developed stable transfected lines of PC12 cells with downregulated expression of neuron-specific PMCA2 (2 line) or PMCA3 (3 line), which have been validated in our several other studies [36, 37]. The most critical finding was permanently increased resting cytosolic  $\text{Ca}^{2+}$  concentration in PMCA-reduced lines due to compromised  $\text{Ca}^{2+}$  extrusion ability observed even despite compensatory stimulation of PMCA1 expression detected in both lines and of PMCA4 in 3 line [36]. We have also provided the evidence that altered PMCA composition may play a role in regulation of bioenergetic function of mitochondria [37, 38]. Moreover, PMCA altered expression of genes encoding a number of elements responsible for regulation of calcium homeostasis [39, 40]. Taking into consideration that decreased amount and activity of PMCA may underlie many neurodegenerative diseases, here we analyzed whether the modified profile of plasma membrane calcium pumps can influence cell response to CCL5-induced signaling.

## 2. Materials and Methods

**2.1. Cell Culture.** Cell culture and differentiation PC12 rat pheochromocytoma cells (ATCC, USA) were routinely maintained in RPMI-1640 medium (Biowest, USA) containing 15% fetal bovine serum (Biowest, USA), 25 mM HEPES,

pH 7.4 (21°C), 2 mM L-glutamine, 25 U/ml penicillin, and 25  $\mu\text{g}/\text{ml}$  streptomycin in a humidified incubator at 37°C with 5%  $\text{CO}_2$ . Stable transfected cell lines with reduced PMCA2 (2) or PMCA3 (3) protein level were achieved using an antisense RNA cloned into pcDNA3.1(+) vector transfected to naive PC12 cells, as described previously [36]. Following selection with increasing G418 concentration (up to 1 mg/ml), the stable transfectants with nearly 50% reduction in PMCA2 or PMCA3 protein level were obtained. PC12 cells carrying an empty vector were used as a control (C). PC12 cells derived from a transplantable rat pheochromocytoma can differentiate into sympathetic-like neuronal cells upon exposure to neurotrophins, but similar effects can be triggered by db-cAMP. In our model differentiation process was induced with 1 mM dibutyryl-cAMP (Santa Cruz Biotechnology) for 48 h. Because PC12 cells exhibit some level of variability, routinely no more than 12 passages were used.

**2.2.  $\text{Ca}^{2+}$  Measurement.** Cells grown to 80% confluence in 25  $\text{cm}^2$  flasks were detached from the surface and centrifuged at low speed (250  $\times$  g) for 5 min. 100  $\mu\text{l}$  of cell suspension was immediately transferred to 96-well plates. An equal volume of 2 $\times$  concentrated Fluo-4 Direct calcium reagent loading solution (Life Technologies, USA) was added to each well and plates were incubated at 37°C for 1 h. Fluorescence was measured by using a Victor X3 plate reader (Perkin-Elmer). The measurements were performed for 250 s at one second intervals at 37°C and the fluorescence signal was recorded using 488 nm excitation filter and 535 nm emission filter. The signal was calibrated by addition of 0.1% Triton X-100 to obtain  $R_{\text{max}}$  and 10 mM EGTA to chelate extracellular  $\text{Ca}^{2+}$  to obtain  $R_{\text{min}}$ . Appropriate controls for estimation of background fluorescence including phenol red free RPMI medium, Fluo-4 solution alone, and cell-free recording solution were included. Changes in fluorescence of Fluo-4 dye were converted to free cytosolic  $\text{Ca}^{2+}$  concentration according to the equation  $[\text{Ca}^{2+}]_{\text{free}} = K_d \cdot ([F - F_{\text{min}}] / [F_{\text{max}} - F])$ , where  $K_d = 345$  nM. All measurements were performed in a calcium-free buffer containing 125 mM NaCl, 5 mM KCl, 1.2 mM  $\text{KH}_2\text{PO}_4$ , 1.2 mM  $\text{MgSO}_4$ , 6 mM glucose, and 25 mM HEPES. In all experiments, after measurement of basal  $\text{Ca}^{2+}$  for 150 s, 50 ng/ml of CCL5 (PeproTech) was added. For analysis of CCR/PLC/ $\text{IP}_3$ R pathway, specific inhibitors were added right before measurements—cocktail of CCRs inhibitors: 1 nM BX513 (Abcam) for CCRI, 1  $\mu\text{M}$  SB328437 (Abcam) for CCR3 and 1 nM DAPTA (Abcam) for CCR5 or 4  $\mu\text{M}$  U73122 (Abcam) for PLC, or 100  $\mu\text{M}$  2-APB (Sigma) for  $\text{IP}_3$ Rs. To determine the role of ER calcium stores in CCL5 response, 1  $\mu\text{M}$  thapsigargin (Santa Cruz Biotechnology) was added 50 s after basal calcium measurement, and next 50 ng/ml of CCL5 at 150 s was applied. All measurements were done in duplicate and the data presented in the figures are the average of at least 5 independent cell cultures.

**2.3. RNA Isolation and Real-Time PCR.** Total cellular RNA was isolated using Tri Reagent (MRC) according to the manufacturer's protocol. 1  $\mu\text{g}$  of purified RNA and oligo(dT) primers were then used for cDNA synthesis using High-Capacity cDNA Reverse Transcription Kit (Applied

Biosystems). The IP<sub>3</sub>R genes expression level was quantified in a real-time PCR reaction using 5x HOT FIRE Pol Eva Green qPCR Mix Plus (Solis Biodyne) in the following conditions: 15 min at 95°C followed by 40 cycles at 95°C for 15 s, 60°C for 30 s, and 72°C for 30 s using ABI Prism 7000 sequence detection system (Applied Biosciences). Following normalization to the expression of endogenous *Gapdh*, the fold change of each target gene was calculated using comparative  $2^{-\Delta\Delta Ct}$  method as described previously [36]. Primers were synthesized in the Institute of Biochemistry and Biophysics (Poland) and their specificity was confirmed by running a melting curve after each reaction. Primers were designed using GenScript Primer Design Tool (USA) and their sequences were as follows:

*Ip3r-1* forward: 5'-GTGGAGGTTTCATCTGCAAGC-3',

reverse: 5'-GCTTTCGTGGAATACTCGGTC-3',

*Ip3r-2* forward: 5'-GCTCTTGCCCTGACATTG-3',

reverse: 5'-CCCATGTCTCCATTCTCATAGC-3',

*Ip3r-3* forward: 5'-AGCGAGAAGCAGAAGAAAG-3',

reverse: 5'-CATCCGTGGGAACCAGTC-3',

*Gapdh* forward: 5'-GCTTACCAG-GGCTGCCTTCT-3',

reverse: 5'-CTTCCCATTTCTCAGCCTTGAC-3'.

**2.4. Western Blotting.** Approximately 40-80 µg of cell lysate proteins were separated using either 8% or 10% SDS-PAGE and electroblotted onto nitrocellulose membranes using semidry method. The membranes were blocked with 3% BSA in TBS buffer (10 mM Tris-HCl, pH=7.4, 150 mM NaCl) for 30 min at room temperature prior to exposure to primary antibodies. Membranes were incubated overnight at 4°C with the primary antibodies and for approximately 4 h with the secondary antibodies at room temperature followed by 3 × 15 min wash with TBS-T between each antibody application. The following primary antibodies were used: anti-CCR1 (rabbit, polyclonal, 1:1000, Santa Cruz Biotechnology; rabbit, polyclonal, 1:1000, BosterBio), anti-CCR3 (rabbit, polyclonal, 1:1000, Santa Cruz Biotechnology; rabbit, monoclonal, 1:1000, BosterBio), anti-CCR5 (mouse, monoclonal, 1:1000, Santa Cruz Biotechnology), anti-IP<sub>3</sub>R-1 (rabbit, polyclonal, 1:2000, Alomone Labs), anti-IP<sub>3</sub>R-2 (rabbit, polyclonal, 1:200, Alomone Labs), monoclonal anti-IP<sub>3</sub>R-3 (mouse, monoclonal, 1:2000, BD Biosciences), and anti-IP<sub>3</sub>R-1/2/3 (mouse, monoclonal, 1:500, Santa Cruz Biotechnology). Monoclonal anti-β-actin antibody (Santa Cruz Biotechnology) was used at 1:1000 dilution as a protein loading control. Secondary antibodies coupled with alkaline phosphatase (Sigma) at 1:5000 dilution were used for staining. Sigma Fast BCIP/NBT was used for visualization according to the manufacturer's instruction. Blots were scanned and band intensities were measured quantitatively using GelDoc™ EQ system with Quantity One 1-D Analysis Software version 4.4.1 (Bio-Rad).

**2.5. Confocal Imaging.** Cells were seeded at a density of  $2 \times 10^4$  cells/well on thin-glass bottomed 96-well plate (Sensoplate™, Greiner Bio-One) and differentiated for 48 h. Next, cell cultures were washed once with PBS and fixed for 10 min in room temperature with 2% formaldehyde freshly prepared from paraformaldehyde and buffered to pH = 7.4 in PBS. Subsequently, cells were washed once and further incubated for 1 h with the blocking buffer (10% normal goat serum, 0.1% Triton X-100, PBS pH = 7.4), following 1 h incubation with primary antibody against CCR5 diluted in the blocking buffer (1:100, Santa Cruz Biotechnology). Next, cells were washed 3 × 5 min with the blocking buffer and incubated for 1 h with secondary goat anti-mouse IgG1 antibody conjugated with Alexa Fluor 488 (1:1000, Thermo Fisher Scientific) to fluorescently label immunodetected CCR5. Subsequently, after 3 × 5 min wash with the blocking buffer, plasma membrane marker protein Na<sup>+</sup>/K<sup>+</sup> ATPase was immunostained for 1 h with primary antibody (Abcam) fluorescently labeled with Zenon™ Alexa Fluor 568 Mouse IgG1 Labeling Kit (Thermo Fisher Scientific) and diluted in the blocking buffer (1:50). Finally, cells were washed 3 × 5 min with the blocking buffer, once with PBS, and were fixed again for 10 min in room temperature with 2% formaldehyde in PBS (pH = 7.4). Eventually, cell nuclei were counterstained with 5 µM Hoechst 33342 in PBS, and triple-stained cells were visualized by confocal microscopy. Images were obtained using 780 LSM confocal microscope (Zeiss) with Plan-Apochromat 63x/1.4 Oil DIC M27 objective. ZEISS Microscope Software ZEN2012 was used to calculate mean fluorescence intensities of respective CCR5-positive pixels colocalizing with plasma membrane marker (Na<sup>+</sup>/K<sup>+</sup> ATPase-positive) pixels. Plasma membrane marker-positive pixels were selected based on their fluorescence intensity that ought to be between arbitrary upper (500 units) and lower (40 units) thresholds, set either to eliminate nonspecific background staining or to negate the influence of high-intensity artificial staining (antibody precipitates and others). Analysis of fluorescence intensity of CCR5 staining colocalizing with plasma membrane staining was performed for each cell line for five different fields of view and results were averaged.

**2.6. Data Analysis.** The data are shown as means ± SD of n separate experiments (n ≥ 3) with the exact n value given under each figure. The comparisons between cell lines were done using Student's *t*-test or ANOVA followed by Tukey or Bonferroni's multiple comparisons tests, wherever applicable. P values were calculated using STATISTICA 12.0 (StatSoft) or GraphPad Prism 7 (GraphPad, La Jolla, CA). P < 0.05 was considered as statistically significant.

### 3. Results

**3.1. CCRs Expression in PC12 Cell Lines.** First, we evaluated the presence of CCR1, CCR3, and CCR5 in PC12 lines using two approaches. The immunoreactivity of examined receptors was initially assayed in a cell lysate by Western blot (Figure 1). In comparison to the control cells, CCR1 was present at higher level in <sub>3</sub> cells, CCR3 increased in <sub>2</sub> cells,

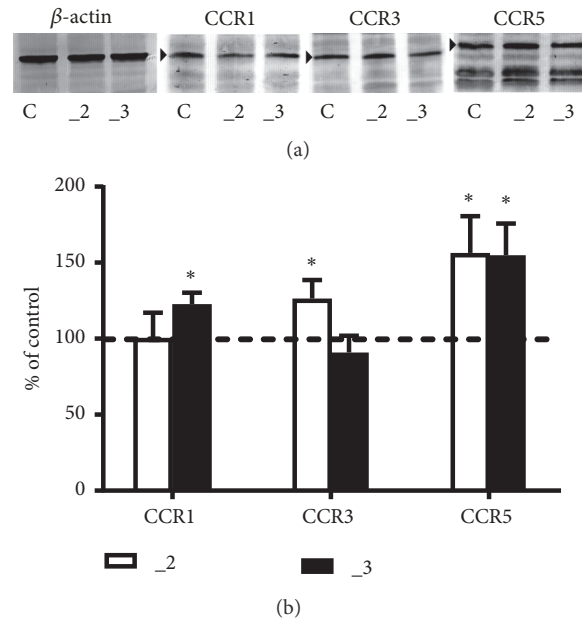


FIGURE 1: Western blot analysis of CCRs protein in PC12 cell lines. (a) Approximately 40–60  $\mu$ g of total protein was resolved on a 10% SDS-PAGE gel and electroblotted onto nitrocellulose membranes. Membranes were probed with polyclonal anti-CCR1, polyclonal anti-CCR3, or monoclonal anti-CCR5. Representative blots are shown and arrows indicate the main band of the receptors with apparent MW 41 kDa for CCR1, 40 kDa for CCR3, and 46 kDa for CCR5. (b) The bands intensity was densitometrically analyzed and the results are expressed as % of the control PC12 cells obtained after normalization to endogenous  $\beta$ -actin level ( $\pm$  SD). \*  $P < 0.05$  ( $n=7$ ), C: control line, \_2: PMCA2-reduced line, \_3: PMCA3-reduced line.

but in both PMCA downregulated PC12 lines CCR5 amount increased by nearly 50%.

Since functionally active chemokine receptors are located at the plasma membranes, we next explored cellular distribution of CCRs by confocal microscopy. Staining of endogenous CCR1 and CCR3 showed low immunosignal intensity, which was concentrated predominantly in the cytosolic area (data not shown). To validate these results, we repeated the assay using another set of antibodies against CCR1 and CCR3; however, we obtained similar results. These data indicated that although CCR1 and CCR3 were present in PC12 cell lines, their participation in CCL5 signaling in our model seems to be negligible. CCR5 was expressed much more abundantly and was mostly distributed in the plasma membranes (Figure 2). Quantification of CCR5 immunofluorescence revealed that cells with reduced PMCA2 or PMCA3 contained more plasma membrane-located receptor than that of control line.

**3.2. CCL5 Effect on Calcium Transients.** To analyze CCL5-induced cytosolic  $Ca^{2+}$  increase in examined PC12 cell lines, chemokine action was assayed in a calcium-free medium to avoid the secondary effect triggered by “calcium-induced calcium release” process, as well as the concomitant participation of membrane calcium channels. Changes in fluorescence were monitored for 250 s at one-second intervals, and CCL5 was always applied after 150 s of measurement. The CCL5 concentration was chosen because it was shown to be effective under inflammatory state, which is supported by literature data. It is also frequently used for *in vitro* assays including PC12 cells [41]. At resting state higher  $Ca^{2+}$

level in PMCA-reduced PC12 cells was observed (Figure 3), confirming our previous results [36].

Treatment with CCL5 at 50 ng/ml increased cytosolic  $Ca^{2+}$  in all examined lines, more intensively in PMCA-modified cells, but the highest peak value was observed in \_2 line. This was also confirmed by analysis of area under the curves. Time course of chemokine effect presented in Figure 4(a) (black lines) showed a fast transient increase in  $[Ca^{2+}]_c$  during first seconds after CCL5 application, followed by a slow, progressive decrease in  $[Ca^{2+}]_c$ . The estimated time required for recovery of  $Ca^{2+}$  to the basal level was  $14 \pm 1$  s for control PC12 cells,  $41 \pm 8^*$  s for \_2 line, and  $23 \pm 7^{*#}$  s for \_3 line ( $n=5$ ; \* $P < 0.05$  vs. control; # $P < 0.05$  \_3 vs. \_2). Slower recovery in \_2 and \_3 lines could result from lowered  $Ca^{2+}$ -clearing potency in PMCA-reduced lines, since SERCA affinity for calcium is at low micromolar range [42]. In  $Ca^{2+}$ -free conditions, the differences in cell response to CCL5 might reflect a balance between intensity of  $Ca^{2+}$  release from ER and  $Ca^{2+}$  extrusion, which varied between cell lines.

To verify that in our experimental conditions the endoplasmic reticulum was a main source of calcium, the assay was performed in the presence of  $1\mu$ M thapsigargin added after 50 s, and next CCL5 was applied at 150 s. As shown in Figure 4(a) (red lines), Tg caused a successive calcium depletion from ER due to inhibition of  $Ca^{2+}$  reuptake by SERCA, and subsequent addition of chemokine had no effect on calcium transient. To confirm the participation of CCRs in generation of  $Ca^{2+}$  transient, the assay was also performed in the presence of specific CCRs inhibitors. Although CCR5

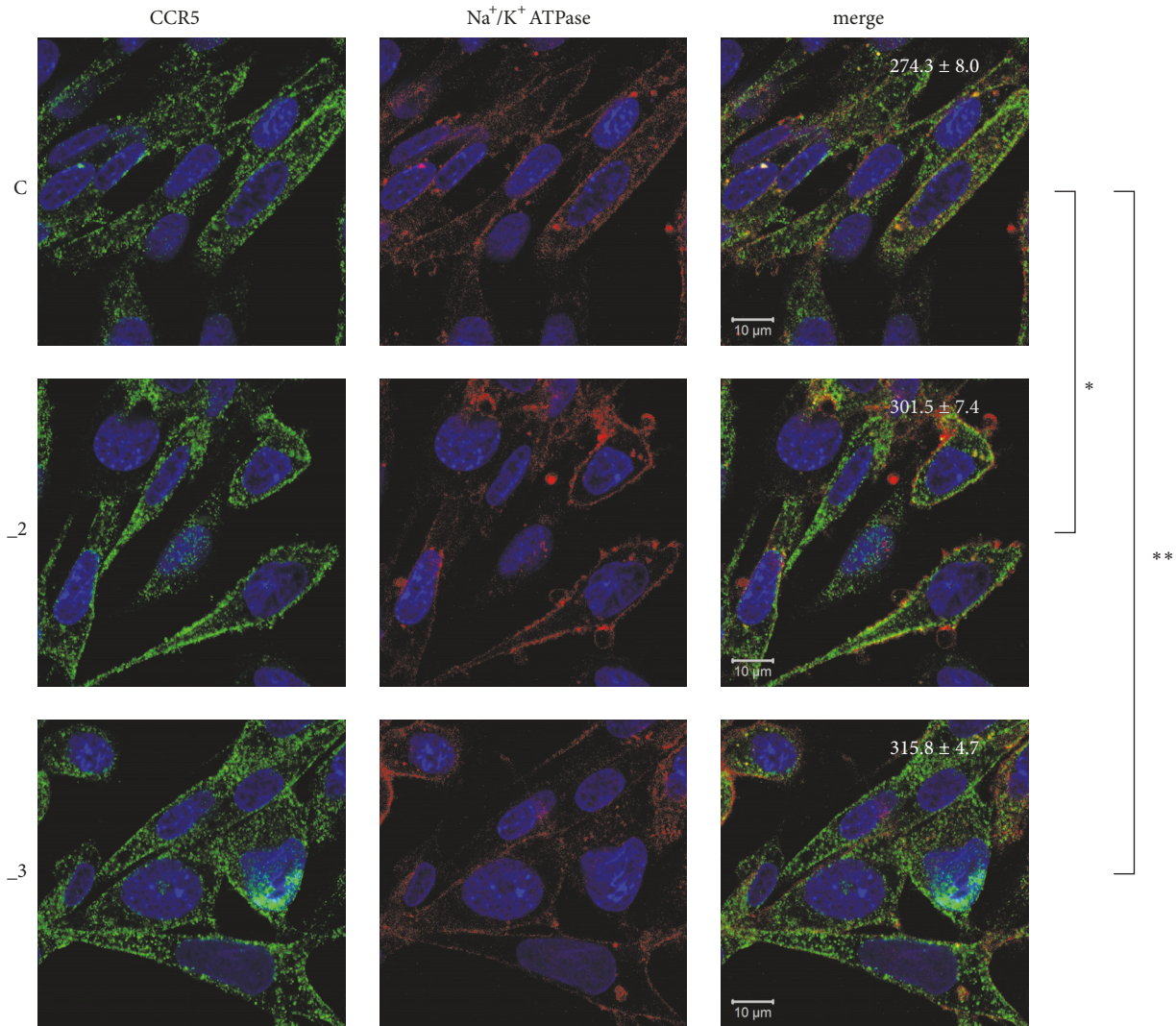


FIGURE 2: Localization of CCR5 in PC12 cell lines. PC12 cells differentiated for 48 h with db-cAMP were fixed and immunostained with antibodies against CCR5 receptor (green) and Na<sup>+</sup>/K<sup>+</sup> ATPase (plasma membrane marker, red). Nuclei were stained with Hoechst 33342 (blue). Representative confocal images are presented. Values shown in merged images represent average fluorescence intensity ± SEM (n = 5) of pixels positive in green channel (CCR5) that colocalize with red channel positive pixels (Na<sup>+</sup>/K<sup>+</sup> ATPase). \* P < 0.05, \*\* P < 0.01. Scale bars: 10 μm. C: control line, \_2: PMCA2-reduced line, \_3: PMCA3-reduced line.

appeared to be the main functionally active receptor in our cell lines, chemokine action was assessed in the presence of cocktail of CCR1, CCR3, and CCR5 inhibitors added just before measurement (Figure 4(b), red lines). CCL5 applied after 150 s did not affect Ca<sup>2+</sup> level indicating that examined CCRs were indeed the crucial targets for the chemokine.

**3.3. Analysis of PLC/IP<sub>3</sub>R Pathway.** In the next step we analyzed the downstream signaling triggered by CCL5/CCR complex by inhibiting the crucial elements of this pathway, PLC and IP<sub>3</sub> receptors. As shown in Figure 5(a) (red lines), in the presence of selective PLC inhibitor, U73122, there was no Ca<sup>2+</sup> response to CCL5 in examined cell lines, which confirmed that PLC-induced signaling must be the chemokine effector. Subsequent generation of a second messenger, IP<sub>3</sub>, leads to the opening of IP<sub>3</sub>-dependent calcium

channels. Thus, we treated cells with 2-APB, an inhibitor of IP<sub>3</sub> receptors (Figure 5(b), red lines). Baseline Ca<sup>2+</sup> level was not affected by the chemokine in these conditions, showing that IP<sub>3</sub>Rs were indeed responsible for observed calcium transients.

**3.4. Characteristics of IP<sub>3</sub> Receptors in PC12 Cell Lines.** Since IP<sub>3</sub> receptors appeared to be the final CCL5 effectors in analyzed pathway, we next characterized their expression in our PC12 cell lines. Real-time PCR analysis showed significant IP<sub>3</sub>R-1 and IP<sub>3</sub>R-2 downregulation in both \_2 and \_3 lines, whereas the expression of IP<sub>3</sub>R-3 increased in comparison to the control cells (Figure 6).

To validate whether the mRNA changes correlated with corresponding receptor protein, Western blot analysis was performed using isoform-specific antibodies and the

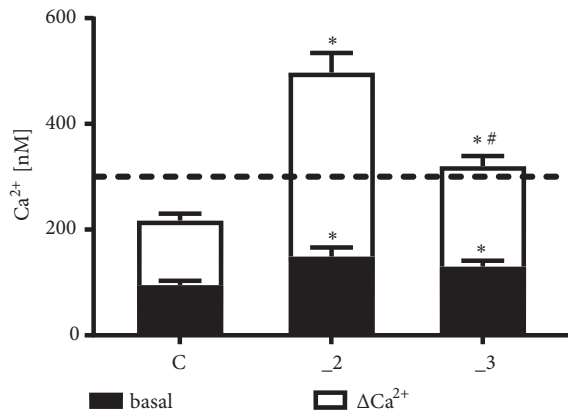


FIGURE 3: CCL5 effect on Ca<sup>2+</sup> release in PC12 cell lines. The maximal level of [Ca<sup>2+</sup>]<sub>c</sub> liberated by 50 ng/ml CCL5 was reached approximately during first seconds after addition of chemokine and was determined as an average of peak values from 5 separate experiments ( $\pm$  SD).  $\Delta$ [Ca<sup>2+</sup>]<sub>c</sub> was calculated by subtracting the resting level (black box) from maximal Ca<sup>2+</sup> concentration. \*  $P < 0.05$  vs. control line, #  $P < 0.05$  \_3 line vs. \_2 line (n=5). \_2: PMCA2-reduced line, \_3: PMCA3-reduced line.

antibody that recognized all three IP<sub>3</sub> receptors (Figure 7(a)). Single bands of the predicted sizes for IP<sub>3</sub>-1, 2, and 3 receptors (~313 kDa, 260 kDa, and 250 kDa, respectively) were detected in all lines, but some lower molecular weight bands were also present. They could represent proteolytic fragments of the receptors, as similar observations were also shown in another study [43].

Quantification of individual IP<sub>3</sub>R isoforms confirmed that in \_2 and \_3 lines the protein level of IP<sub>3</sub>R-1 and 2 was lower than that of control cells, but IP<sub>3</sub>R-3 increased by ~40% (Figure 7(b)). However, analysis of blots probed with antibody recognizing all IP<sub>3</sub> receptors revealed a total increase only in \_3 line. This apparently indicates the differences in a ratio between IP<sub>3</sub>R isoforms and finally could result in diversified affinity for IP<sub>3</sub> in both PMCA-reduced cell lines.

#### 4. Discussion

Our previous studies revealed that, in differentiated PC12 cells, downregulation of neurospecific PMCA2 or PMCA3 increased cytosolic Ca<sup>2+</sup> and subsequently affected the expression level of several Ca<sup>2+</sup>-associated proteins, i.e., SERCA, calmodulin, calcineurin, neuromodulin (GAP43), and certain types of voltage-gated calcium channels [36, 39, 40]. We have also revealed a compensatory increase of PMCA1 isoform in both PMCA-reduced lines coexisting with higher expression of SERCA2 and SERCA3, which correlated with higher Ca<sup>2+</sup> accumulation in the endoplasmic reticulum [36]. On the one hand it could effectively decrease cytosolic Ca<sup>2+</sup> concentration to its safe level, but on the other hand, it may potentially increase Ca<sup>2+</sup> release after activation of calcium channels in the ER, including activation of IP<sub>3</sub> receptors and ryanodine receptors [42]. Since IP<sub>3</sub>R-mediated Ca<sup>2+</sup> release from the ER and mitochondrial Ca<sup>2+</sup> homeostasis

are physiologically coupled, their improper cooperation may significantly affect cell viability [44].

Based on current study, we can add to the list of common features detected after reduction of PMCA2 or PMCA3 increased level of CCR5 and IP<sub>3</sub>R-3 proteins, but lowered IP<sub>3</sub>R-1 and IP<sub>3</sub>R-2. All these changes are primarily related to elevated cytosolic Ca<sup>2+</sup> as a consequence of changed composition of PMCA. Interestingly, some of them could occur as adaptive processes protecting cells against calcium overload. Since age-related PMCA decrease has been documented [17, 45–47], our modified PC12 cells may be a useful model to clarify the biological changes in neurons associated with aging and, potentially, to study the vulnerability of cells to neurodegenerative insults.

The presence of CCR5 in PC12 cells was shown in several studies [25, 41], and it was also confirmed by our data. Moreover, we detected CCR1 and CCR3 proteins, but their cytosolic localization suggested that CCL5 signal was mainly transmitted by CCR5, because the activity of receptor requires its presence in the plasma membrane. Upregulation of CCR5 has been revealed in a number of neurological disorders and models of CNS injury, where it is often localized in astrocytes and microglial cells [48–51]. Overactivation of CCR5 with subsequent raise of cytosolic Ca<sup>2+</sup> affected chemotaxis, secretion, and gene expression and could lead to inflammatory and degenerative processes in the CNS [27, 29]. Chemokine receptors could bind several chemokines and could act as multimeric forms, homo- or heterodimers [52–55]. The additional mechanism that may modify CCL5 signaling depends on the function of another type of calcium channels existing in ER, ryanodine receptors. RyRs are activated by a mechanism known as Ca<sup>2+</sup>-induced Ca<sup>2+</sup> release (CICR) and involve cooperation with plasma membrane calcium channels [56]. Crucial for RyRs function is a high, micromolar Ca<sup>2+</sup> concentration necessary to open these channels [57]. In our study, to avoid the potential influence of RyR-mediated secondary effects, we assayed CCL5 action without external calcium.

Using the selected inhibitors we confirmed that in our cell models CCL5 downstream effects involved CCR5-PLC-IP<sub>3</sub>R pathway. The crucial step appeared to be associated with activation of IP<sub>3</sub> receptors. Although IP<sub>3</sub>R-1 represents a predominant isoform in the central nervous system, other isoforms also exist in some brain areas and may differ in neuronal compartmentalization [58–60]. A particular role of IP<sub>3</sub>R in hippocampus is related to learning and memory abilities, and changes in IP<sub>3</sub>R isoforms composition during aging may have an impact on increased deficits in these processes. In most cultured cell types IP<sub>3</sub>R-3 is the principal form, but IP<sub>3</sub>R-1 and IP<sub>3</sub>R-2 have also been detected [61]. All isoforms exhibit specific characteristics: IP<sub>3</sub>R-1 possesses low Ca<sup>2+</sup> affinity and medium affinity for IP<sub>3</sub>, IP<sub>3</sub>R-2 represents the isoform with the highest affinity for both Ca<sup>2+</sup> and IP<sub>3</sub>, and IP<sub>3</sub>R-3 is the most sensitive for modulation by Ca<sup>2+</sup>, but displays the lowest IP<sub>3</sub> affinity [60]. Interestingly, IP<sub>3</sub>R are regulated in a biphasic way by cytosolic Ca<sup>2+</sup> and are stimulated at low Ca<sup>2+</sup> level, but inhibited by higher than 300 nM Ca<sup>2+</sup> [33]. Up to now, over 100 proteins have

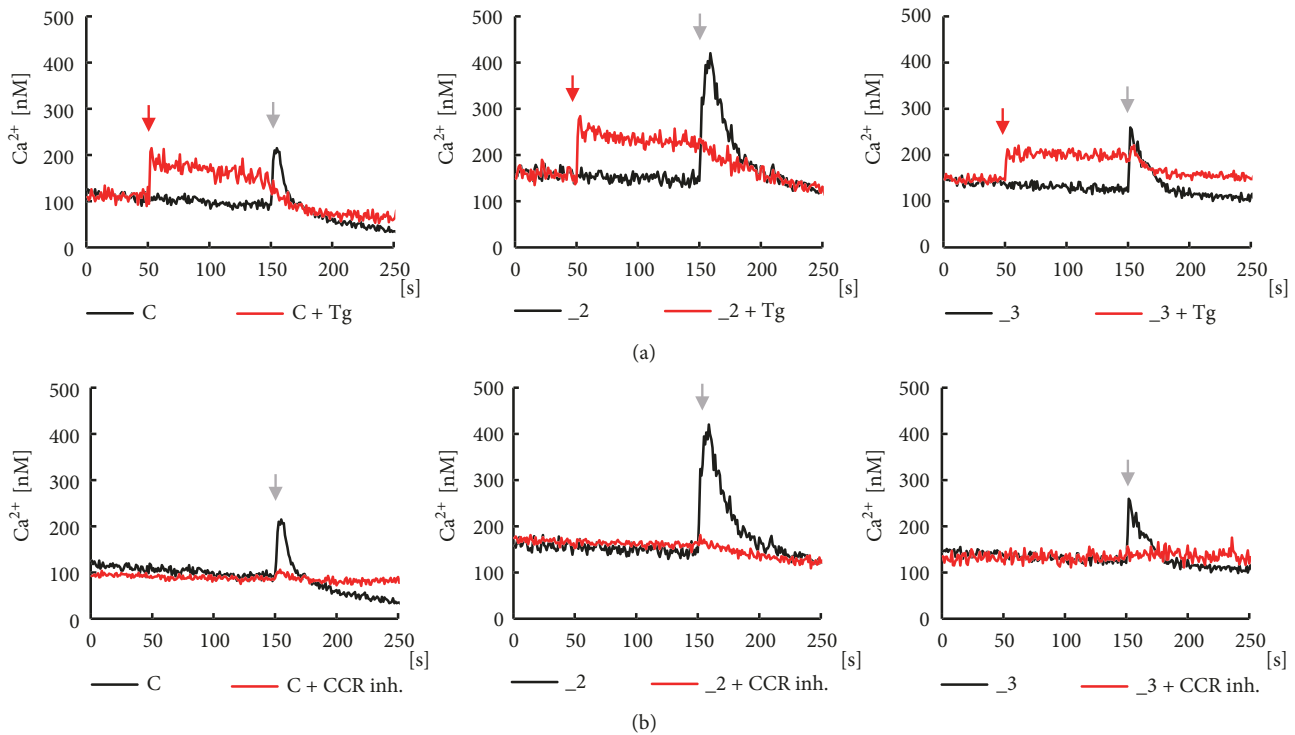


FIGURE 4: Analysis of CCL5 effect on calcium transients in PC12 cell lines.  $\text{Ca}^{2+}$  transients were measured in parallel wells with (red lines) or without (black lines) presence of specific inhibitors. (a) SERCA inhibitor,  $1\mu\text{M}$  thapsigargin, was added after 50 s (red arrow), and next 50 ng/ml CCL5 was applied after 150 s (black arrow). (b) CCRs inhibitors, 1 nM BX513 for CCR1,  $1\mu\text{M}$  SB328437 for CCR3, and 1 nM DAPTA for CCR5, were included just before measurements. 50 ng/ml CCL5 was applied after 150 s (black arrow). All measurements were done in duplicate and the presented traces are average from 5 independent cell cultures ( $n=10$ ). C: control line,  $\_2$ : PMCA2-reduced line,  $\_3$ : PMCA3-reduced line.

been identified to interact with and regulate the  $\text{IP}_3\text{Rs}$  [62]. Thus, multiple regulatory processes for each  $\text{IP}_3\text{R}$  isoform may produce diversified cell signaling paths that can initiate the adaptive response or can lead to neurodegeneration [60, 61].

Our analysis showed that in PC12 cells, all three  $\text{IP}_3\text{R}$  isoforms were present, with  $\text{IP}_3\text{R-3}$  being the most prominent subtype. An interesting observation made here was the altered composition of  $\text{IP}_3\text{Rs}$  in PMCA-reduced lines at both mRNA and protein level.  $\text{IP}_3\text{R-1}$  and  $\text{IP}_3\text{R-2}$  decreased, whereas  $\text{IP}_3\text{R-3}$  amount was higher than that of control cells. Changes in relative mRNA level indicate that the regulation occurs at the level of transcription, suggesting  $\text{Ca}^{2+}$ -dependent negative feedback loop for  $\text{IP}_3\text{R-1}$  and  $\text{IP}_3\text{R-2}$ . Analysis of  $\text{IP}_3\text{R}$  protein levels also confirmed the differences in a ratio of  $\text{IP}_3\text{R}$  isoforms between control  $\_2$  and  $\_3$  lines. One can assume that in both PMCA-reduced cells the decreased expression of receptors with higher affinity for  $\text{IP}_3$  could lower the total apparent sensitivity to  $\text{IP}_3$  and thereby may provide some protection against calcium overload. The graphical summary of these findings is presented in Figure 8.

In  $\_2$  line, we observed higher  $\text{Ca}^{2+}$  accumulation in the ER; thus potentially more calcium could be released after activation of  $\text{IP}_3\text{Rs}$ . Moreover, less efficient PMCA-dependent extrusion system, due to PMCA2 suppression, may prolong calcium signaling, modifying a number of existing pathways. It can also lead to further  $\text{Ca}^{2+}$  overload. In fact, in this line we

reported decreased cell survival and increased percentage of apoptotic cells [36]; thus the cells may exhibit higher vulnerability to calcium-induced cytotoxicity. Correlation between PMCA2 and disturbances in cell function resulting in augmented cell death has been reported in neurons, indicating a protective PMCA2 role [13, 63]. Taking into account the fact that PMCA2 represents nearly 40% of the total pump in the brain [64], reduction of PMCA2 appears to be more harmful for the cells than deficiency of PMCA3, and compensatory mechanisms may not be sufficient for full protection of cells.

The presence of an additional protective mechanism may be suggested in the  $\_3$  line, where we previously observed increased expression of PMCA4 isoform. One of the well-established mechanisms of PMCA regulation is stimulatory action of  $\text{PIP}_2$  [9, 65, 66]. Recently, a new look on PMCA/ $\text{PIP}_2$  interaction has been proposed [67]. Binding of  $\text{PIP}_2$  by PMCA4 has been demonstrated to protect plasma membrane  $\text{PIP}_2$  from hydrolysis by PLC. It could potentially limit  $\text{IP}_3$  production and, subsequently, restrict  $\text{Ca}^{2+}$  release from ER. Since for full activity,  $\text{IP}_3\text{Rs}$  must bind four  $\text{IP}_3$  molecules [68], a sufficient available  $\text{PIP}_2$  concentration as a substrate for PLC is a necessary requirement. Accordingly, in the  $\_3$  line greater protection could result not only from the altered profile of  $\text{IP}_3\text{Rs}$  and the presence of highly active PMCA2, but also from higher PMCA4 amount. All these adaptive changes may limit the amount of  $\text{Ca}^{2+}$  released from

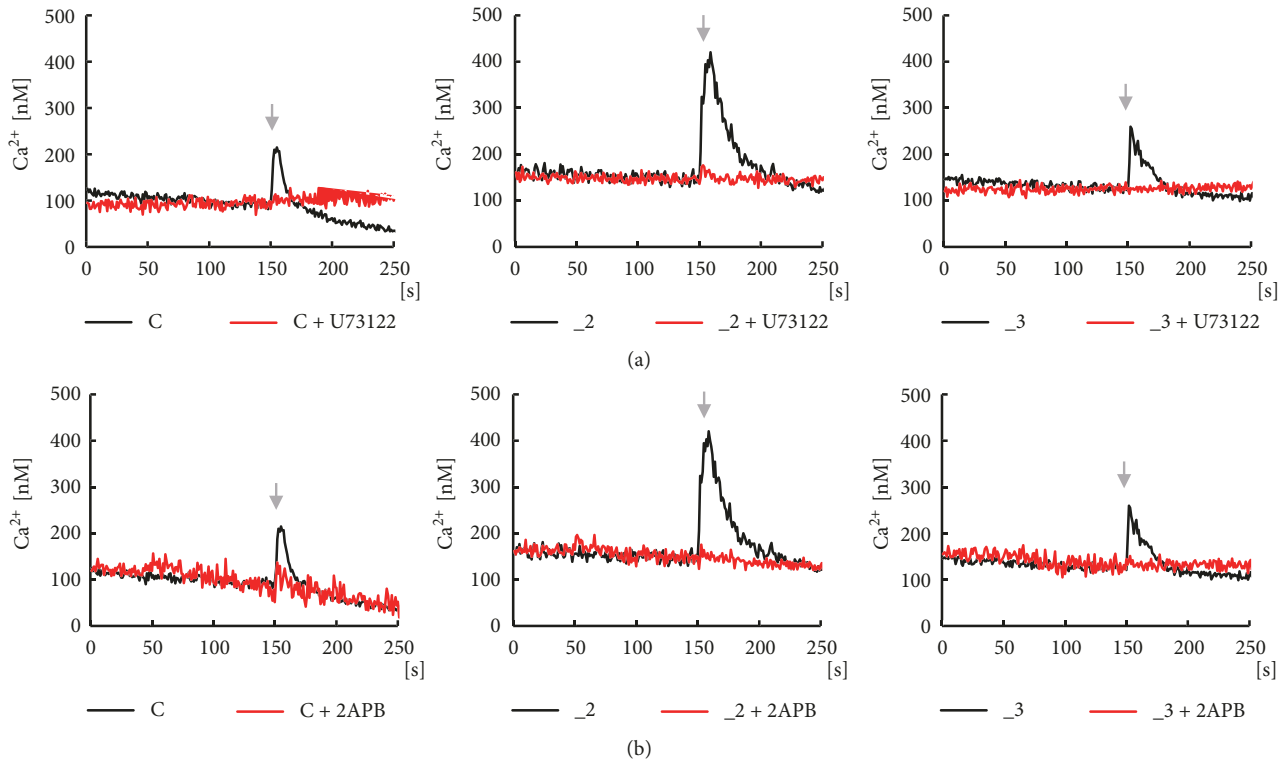


FIGURE 5: Analysis of PLC/IP<sub>3</sub>R signaling pathway in PC12 cell lines. Analysis of PLC/IP<sub>3</sub>R pathway was performed in parallel wells with (red lines) or without (black lines) presence of specific inhibitors included just before measurements. 50 ng/ml CCL5 was always applied after 150 s (black arrow). The calcium transients were assayed in the presence of (a) PLC inhibitor, 4  $\mu$ M U73122, and (b) IP<sub>3</sub>Rs inhibitor, 100  $\mu$ M 2-APB. All measurements were done in duplicate and the presented traces are average from 5 independent cell cultures (n=10). C: control line, 2: PMCA2-reduced line, 3: PMCA3-reduced line.

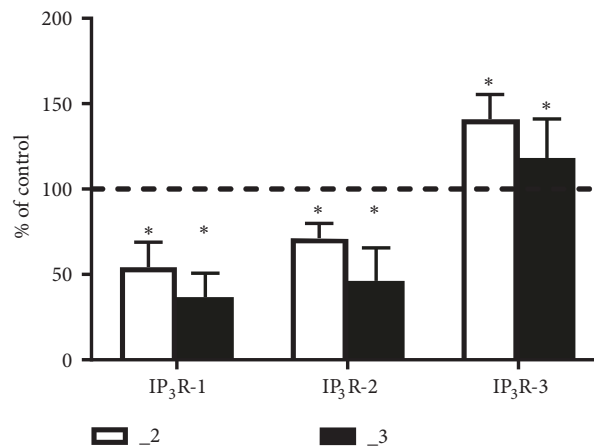


FIGURE 6: Real-time PCR analysis of IP<sub>3</sub> receptors in PC12 cell lines. A relative fold change ( $\pm$  SD) obtained following normalization to *Gapdh* expression and calculated using comparative  $2^{-\Delta\Delta Ct}$  method. The expression of a target gene in control PC12 cells was taken as 100% and is presented as a dotted line. Statistical differences from values in control are indicated by \*P < 0.05 (n = 6). C: control line, 2: PMCA2-reduced line, 3: PMCA3-reduced line.

the ER and shorten the time necessary to restore basal  $Ca^{2+}$  level.

## 5. Conclusions

Downregulation of neuron-specific PMCA2 or PMCA3 initiated a set of responses that significantly altered  $Ca^{2+}$ -induced

signaling that may allow cells to survive but also may promote cell death. The unique role played by “fast” isoforms of plasma membrane calcium pump in neuronal cells suggests that long-lasting calcium dyshomeostasis could markedly increase cell vulnerability to pathological events, including neurodegenerative disorders [13, 19, 63]. Aberration in the activity of PMCA2 has been implicated in some diseases,

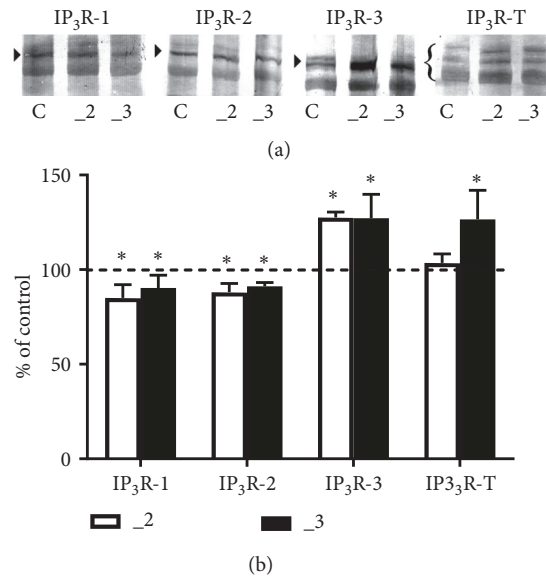


FIGURE 7: Western blot analysis of IP<sub>3</sub> receptors in PC12 cell lines. (a) Approximately 60–80 μg of total protein was resolved on an 8% SDS-PAGE gel and electroblotted onto nitrocellulose membranes. Membranes were probed with anti-IP<sub>3</sub>R1, anti-IP<sub>3</sub>R2, anti-IP<sub>3</sub>R3, and recognizing all isoforms anti-IP<sub>3</sub>R-T antibodies. Representative blots are shown and arrows indicate the main band of the receptors. (b) Band intensity was densitometrically analyzed and the results are expressed as % (± SD) of control PC12 cells obtained after normalization to endogenous β-actin level. \*P < 0.05 (n=7). C: control line, \_2: PMCA2-reduced line, \_3: PMCA3-reduced line.

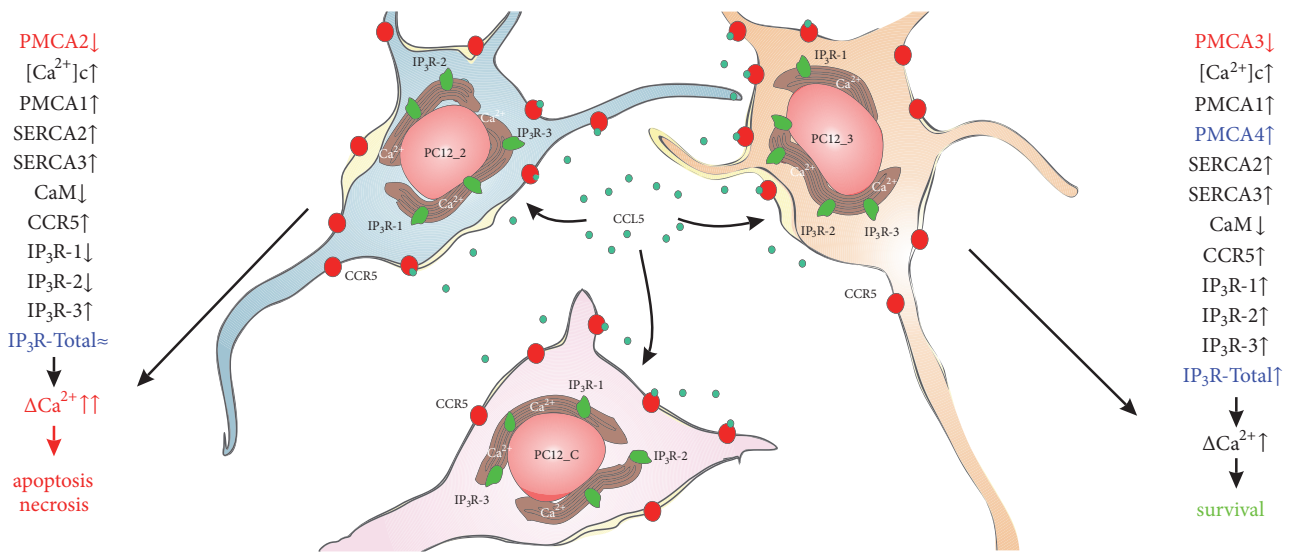


FIGURE 8: Schematic presentation of CCL5 effect on PC12 cells. Downregulation of neurospecific PMCA2 or PMCA3 isoforms in differentiated PC12 cells generated two types of cell response: similar for both lines or characteristic for only one line. The common changes were increased cytosolic Ca<sup>2+</sup> and, as a compensatory mechanism, upregulation of PMCA1 isoform, enlarged expression of SERCA2 and SERCA3, and diminished calmodulin amount [36, 40]. The levels of CCR5 and IP<sub>3</sub>R-3 proteins also increased, but the expression of IP<sub>3</sub>R-1 and IP<sub>3</sub>R-2 was lowered (present study). Interestingly, altered IP<sub>3</sub>R isoform composition did not change total IP<sub>3</sub>R protein in the \_2 line, while it increased in the \_3 line. Also in \_3 cells, the amount of PMCA4 increased [36]. These subtle differences could have profound consequences after CCL5/CCR5 activation, since potency to restore the basal Ca<sup>2+</sup> level in the \_3 line appears to be higher than in the \_2 line, which may be essential for the survival of the cell. Under prolonged Ca<sup>2+</sup> signal in the \_2 line due to reduction of the fastest isoform - PMCA2, the subsequent Ca<sup>2+</sup>-mediated processes could increase vulnerability to cell death. Abbreviations used: CaM, calmodulin; CCL5, chemokine C-C motif ligand 5; CCR5, receptor for CCL5; inositol 1,4,5-triphosphate (IP<sub>3</sub>); IP<sub>3</sub>R, IP<sub>3</sub> receptor; PMCA, plasma membrane Ca<sup>2+</sup>-ATPase; SERCA, sarco/endoplasmic Ca<sup>2+</sup>-ATPase.

i.e., Huntington's disease and multiple sclerosis, but altered expression of PMCA3 has been linked with cerebellar ataxia [69]. Here we demonstrated that CCL5/CCR5 signaling could be one of the critical mediators of the cell fate. Although we analyzed only the initial step in CCL5-induced pathway, this key phase could play a decisive role for the cell. In the aging brain increased BBB permeability, augmented leukocyte infiltration, and more severe CCL5 action under less efficient neuronal  $\text{Ca}^{2+}$  extrusion mechanism could accumulate potentially harmful changes in neurons, which increase the risk of developing neurodegenerative diseases.

## Data Availability

All of data used to support the findings of this study are included within the article.

## Conflicts of Interest

The authors declare that the research was conducted in the absence of any commercial or financial relationships that could be construed as potential conflicts of interest.

## Authors' Contributions

Tomasz Radzik, Tomasz Boczek, Maciej Studzian, Lukasz Pulaski, and Ludmila Zylinska participated in research design and wrote, or contributed to the writing of, the manuscript; Tomasz Radzik, Bozena Ferenc, Maciej Studzian, and Lukasz Pulaski conducted the experiments; Tomasz Radzik, Tomasz Boczek, Maciej Studzian, Lukasz Pulaski, and Ludmila Zylinska performed data analysis.

## Acknowledgments

This work was supported by grants nos. 503/6-086-02/503-61-001 and 502-03/6-086-02/502-64-086 from Medical University of Lodz, Poland. Tomasz Boczek is supported by "Mobility Plus" grant funded by the Polish Ministry of Science and Higher Education.

## References

- [1] L. Cartier, O. Hartley, M. Dubois-Dauphin, and K.-H. Krause, "Chemokine receptors in the central nervous system: role in brain inflammation and neurodegenerative diseases," *Brain Research Reviews*, vol. 48, no. 1, pp. 16–42, 2005.
- [2] J. Chen, R. Mo, P. A. Lescure et al., "Aging is associated with increased T-cell chemokine expression in C57Bl/6 mice," *The Journals of Gerontology. Series A, Biological Sciences and Medical Sciences*, vol. 58, no. 11, pp. B975–B983, 2003.
- [3] A. Chou, K. Krukowski, J. M. Morganti, L.-K. Riparip, and S. Rosi, "Persistent infiltration and impaired response of peripherally-derived monocytes after traumatic brain injury in the aged brain," *International Journal of Molecular Sciences*, vol. 19, no. 6, 2018.
- [4] H. N. Frazier, S. Maimaiti, K. L. Anderson et al., "Calcium's role as nuanced modulator of cellular physiology in the brain," *Biochemical and Biophysical Research Communications*, vol. 483, no. 4, pp. 981–987, 2017.
- [5] S. Orrenius, B. Zhivotovsky, and P. Nicotera, "Regulation of cell death: the calcium-apoptosis link," *Nature Reviews Molecular Cell Biology*, vol. 4, no. 7, pp. 552–565, 2003.
- [6] E. Pchitskaya, E. Popugaeva, and I. Bezprozvanny, "Calcium signaling and molecular mechanisms underlying neurodegenerative diseases," *Cell Calcium*, vol. 70, pp. 87–94, 2018.
- [7] D. M. Sama and C. M. Norris, "Calcium dysregulation and neuroinflammation: Discrete and integrated mechanisms for age-related synaptic dysfunction," *Ageing Research Reviews*, vol. 12, no. 4, pp. 982–995, 2013.
- [8] E. Carafoli, "Calcium pump of the plasma membrane," *Physiological Reviews*, vol. 71, no. 1, pp. 129–153, 1991.
- [9] R. Lopreiato, M. Giacomello, and E. Carafoli, "The plasma membrane calcium pump: new ways to look at an old enzyme," *The Journal of Biological Chemistry*, vol. 289, no. 15, pp. 10261–10268, 2014.
- [10] E. E. Strehler, "Plasma membrane calcium ATPases: From generic  $\text{Ca}^{2+}$  sump pumps to versatile systems for fine-tuning cellular  $\text{Ca}^{2+}$ ," *Biochemical and Biophysical Research Communications*, vol. 460, no. 1, pp. 26–33, 2015.
- [11] E. E. Strehler and D. A. Zacharias, "Role of alternative splicing in generating isoform diversity among plasma membrane calcium pumps," *Physiological Reviews*, vol. 81, no. 1, pp. 21–50, 2001.
- [12] A. Kumar, J. R. Gibbs, A. Beilina et al., "Age-associated changes in gene expression in human brain and isolated neurons," *Neurobiology of Aging*, vol. 34, no. 4, pp. 1199–1209, 2013.
- [13] M. P. Kurnellas, H. Li, M. R. Jain et al., "Reduced expression of plasma membrane calcium ATPase 2 and collapsin response mediator protein 1 promotes death of spinal cord neurons," *Cell Death & Differentiation*, vol. 17, no. 9, pp. 1501–1510, 2010.
- [14] K. Pászty, A. K. Verma, R. Padányi, A. G. Filoteo, J. T. Penniston, and Á. Enyedi, "Plasma membrane  $\text{Ca}^{2+}$  ATPase isoform 4b is cleaved and activated by caspase-3 during the early phase of apoptosis," *The Journal of Biological Chemistry*, vol. 277, no. 9, pp. 6822–6829, 2002.
- [15] E. E. Strehler and S. A. Thayer, "Evidence for a role of plasma membrane calcium pumps in neurodegenerative disease: recent developments," *Neuroscience Letters*, vol. 663, pp. 39–47, 2018.
- [16] B. L. Schwab, D. Guerini, C. Didszun et al., "Cleavage of plasma membrane calcium pumps by caspases: a link between apoptosis and necrosis," *Cell Death & Differentiation*, vol. 9, no. 8, pp. 818–831, 2002.
- [17] A. Zaidi, J. Gao, T. C. Squier, and M. L. Michaelis, "Age-related decrease in brain synaptic membrane  $\text{Ca}^{2+}$ -ATPase in F344/BNF1 rats," *Neurobiology of Aging*, vol. 19, no. 5, pp. 487–495, 1998.
- [18] M. Berrocal, I. Corbacho, M. Vázquez-Hernández, J. Ávila, M. R. Sepúlveda, and A. M. Mata, "Inhibition of PMCA activity by tau as a function of aging and Alzheimer's neuropathology," *Biochimica et Biophysica Acta (BBA) - Molecular Basis of Disease*, vol. 1852, no. 7, pp. 1465–1476, 2015.
- [19] M. Brini, E. Carafoli, and T. Cali, "The plasma membrane calcium pumps: focus on the role in (neuro)pathology," *Biochemical and Biophysical Research Communications*, vol. 483, no. 4, pp. 1116–1124, 2017.
- [20] P. Hajieva, M. W. Baeken, and B. Moosmann, "The role of Plasma Membrane Calcium ATPases (PMCAs) in neurodegenerative disorders," *Neuroscience Letters*, vol. 663, pp. 29–38, 2018.

- [21] V. Khariv and S. Elkabes, "Contribution of Plasma Membrane Calcium ATPases to neuronal maladaptive responses: Focus on spinal nociceptive mechanisms and neurodegeneration," *Neuroscience Letters*, vol. 663, pp. 60–65, 2018.
- [22] G. Zanni, T. Cali, V. M. Kalscheuer et al., "Mutation of plasma membrane Ca<sup>2+</sup> ATPase isoform 3 in a family with X-linked congenital cerebellar ataxia impairs Ca<sup>2+</sup> homeostasis," *Proceedings of the National Academy of Sciences of the United States of America*, vol. 109, no. 36, pp. 14514–14519, 2012.
- [23] M. R. Pranzatelli, "Advances in biomarker-guided therapy for pediatric- and adult-onset neuroinflammatory disorders: targeting chemokines/cytokines," *Frontiers in Immunology*, vol. 9, p. 557, 2018.
- [24] L. A. Campbell, V. Avdoshina, S. Rozzi, and I. Mocchetti, "CCL5 and cytokine expression in the rat brain: differential modulation by chronic morphine and morphine withdrawal," *Brain, Behavior, and Immunity*, vol. 34, pp. 130–140, 2013.
- [25] M. H. Park, Y. K. Lee, Y. H. Lee et al., "Chemokines released from astrocytes promote chemokine receptor 5-mediated neuronal cell differentiation," *Experimental Cell Research*, vol. 315, no. 16, pp. 2715–2726, 2009.
- [26] M. F. Lanfranco, I. Mocchetti, M. P. Burns, and S. Villapol, "Glial- and neuronal-specific expression of CCL5 mRNA in the rat brain," *Frontiers in Neuroanatomy*, vol. 11, p. 137, 2018.
- [27] C. R. Balistreri, C. Caruso, M. P. Grimaldi et al., "CCR5 receptor biologic and genetic implications in age-related diseases," *Annals of the New York Academy of Sciences*, vol. 1100, pp. 162–172, 2007.
- [28] K. Gamo, S. Kiryu-Seo, H. Konishi et al., "G-protein-coupled receptor screen reveals a role for chemokine receptor CCR5 in suppressing microglial neurotoxicity," *The Journal of Neuroscience*, vol. 28, no. 46, pp. 11980–11988, 2008.
- [29] J.-P. Louboutin and D. S. Strayer, "Relationship between the chemokine receptor CCR5 and microglia in neurological disorders: consequences of targeting CCR5 on neuroinflammation, neuronal death and regeneration in a model of epilepsy," *CNS & Neurological Disorders: Drug Targets*, vol. 12, no. 6, pp. 815–829, 2013.
- [30] Y. Takeshita and R. M. Ransohoff, "Inflammatory cell trafficking across the blood-brain barrier: Chemokine regulation and in vitro models," *Immunological Reviews*, vol. 248, no. 1, pp. 228–239, 2012.
- [31] G. C. Wang and V. Casolaro, "Immunologic changes in frail older adults," *Translational Medicine @ UniSa*, vol. 9, pp. 1–6, 2014.
- [32] R. E. Marques, R. Guabiraba, R. C. Russo, and M. M. Teixeira, "Targeting CCL5 in inflammation," *Expert Opinion on Therapeutic Targets*, vol. 17, no. 12, pp. 1439–1460, 2013.
- [33] M. J. Berridge, "The inositol trisphosphate/calcium signaling pathway in health and disease," *Physiological Reviews*, vol. 96, no. 4, pp. 1261–1296, 2016.
- [34] M. Iwai, T. Michikawa, I. Bosanac, M. Ikura, and K. Mikoshiba, "Molecular basis of the isoform-specific ligand-binding affinity of inositol 1,4,5-trisphosphate receptors," *The Journal of Biological Chemistry*, vol. 282, no. 17, pp. 12755–12764, 2007.
- [35] J. B. Parys and H. De Smedt, "Inositol 1,4,5-trisphosphate and its receptors," *Advances in Experimental Medicine and Biology*, vol. 740, pp. 255–279, 2012.
- [36] T. Boczek, M. Lisek, A. Kowalski et al., "Downregulation of PMCA2 or PMCA3 reorganizes Ca<sup>2+</sup> handling systems in differentiating PC12 cells," *Cell Calcium*, vol. 52, no. 6, pp. 433–444, 2012.
- [37] T. Boczek, M. Lisek, B. Ferenc et al., "Plasma membrane Ca<sup>2+</sup>-ATPase isoforms composition regulates cellular pH homeostasis in differentiating PC12 cells in a manner dependent on cytosolic Ca<sup>2+</sup> elevations," *PLoS ONE*, vol. 9, no. 7, Article ID e102352, 2014.
- [38] T. Boczek, M. Lisek, B. Ferenc et al., "Silencing of Plasma Membrane Ca<sup>2+</sup>-ATPase Isoforms 2 and 3 Impairs Energy Metabolism in Differentiating PC12 Cells," *BioMed Research International*, vol. 2014, Article ID 735106, 13 pages, 2014.
- [39] T. Boczek, B. Ferenc, M. Lisek, and L. Zylinska, "Regulation of GAP43/calmodulin complex formation via calcineurin-dependent mechanism in differentiated PC12 cells with altered PMCA isoforms composition," *Molecular and Cellular Biochemistry*, vol. 407, no. 1-2, pp. 251–262, 2015.
- [40] T. Boczek, M. Lisek, B. Ferenc, and L. Zylinska, "Cross talk among PMCA, calcineurin and NFAT transcription factors in control of calmodulin gene expression in differentiating PC12 cells," *Biochimica et Biophysica Acta - Gene Regulatory Mechanisms*, vol. 1860, no. 4, pp. 502–515, 2017.
- [41] H. Tokami, T. Ago, H. Sugimori et al., "RANTES has a potential to play a neuroprotective role in an autocrine/paracrine manner after ischemic stroke," *Brain Research*, vol. 1517, pp. 122–132, 2013.
- [42] E. R. Chemaly, L. Troncone, and D. Lebeche, "SERCA control of cell death and survival," *Cell Calcium*, vol. 69, pp. 46–61, 2018.
- [43] L. Wang, K. J. Alzayady, and D. I. Yule, "Proteolytic fragmentation of inositol 1,4,5-trisphosphate receptors: a novel mechanism regulating channel activity?" *The Journal of Physiology*, vol. 594, no. 11, pp. 2867–2876, 2016.
- [44] S. Marchi, S. Patergnani, S. Missiroli et al., "Mitochondrial and endoplasmic reticulum calcium homeostasis and cell death," *Cell Calcium*, vol. 69, pp. 62–72, 2018.
- [45] L. Jiang, M. D. Bechtel, N. A. Galeva, T. D. Williams, E. K. Michaelis, and M. L. Michaelis, "Decreases in plasma membrane Ca<sup>2+</sup>-ATPase in brain synaptic membrane rafts from aged rats," *Journal of Neurochemistry*, vol. 123, no. 5, pp. 689–699, 2012.
- [46] A. M. Mata, "Plasma membrane Ca<sup>2+</sup>-ATPases in the nervous system during development and ageing," *World Journal of Biological Chemistry*, vol. 1, no. 7, pp. 229–234, 2010.
- [47] A. Zaidi, M. Adewale, L. McLean, and P. Ramlow, "The plasma membrane calcium pumps—the old and the new," *Neuroscience Letters*, vol. 663, pp. 12–17, 2018.
- [48] U. De Fanis, G. C. Wang, N. S. Fedarko, J. D. Walston, V. Casolaro, and S. X. Leng, "T-lymphocytes expressing CC chemokine receptor-5 are increased in frail older adults," *Journal of the American Geriatrics Society*, vol. 56, no. 5, pp. 904–908, 2008.
- [49] K. Grabert, T. Michoel, M. H. Karavolos et al., "Microglial brain regiona dependent diversity and selective regional sensitivities to aging," *Nature Neuroscience*, vol. 19, no. 3, pp. 504–516, 2016.
- [50] A. Salminen, J. Ojala, K. Kaarniranta, A. Haapasalo, M. Hiltunen, and H. A. Soininen, "Astrocytes in the aging brain express characteristics of senescence-associated secretory phenotype," *European Journal of Neuroscience*, vol. 34, no. 1, pp. 3–11, 2011.
- [51] R. L. Yung and M. O. Ruran, "Aging is associated with increased human T Cell CC chemokine receptor gene expression," *Journal of Interferon & Cytokine Research*, vol. 23, no. 10, pp. 575–582, 2003.
- [52] L. D. Bennett, J. M. Fox, and N. Signoret, "Mechanisms regulating chemokine receptor activity," *The Journal of Immunology*, vol. 134, no. 3, pp. 246–256, 2011.

- [53] C. E. Hughes and R. J. B. Nibbs, "A guide to chemokines and their receptors," *FEBS Journal*, vol. 285, no. 16, pp. 2944–2971, 2018.
- [54] M. Mellado, J. M. Rodríguez-Frade, A. J. Vila-Coro et al., "Chemokine receptor homo- or heterodimerization activates distinct signaling pathways," *EMBO Journal*, vol. 20, no. 10, pp. 2497–2507, 2001.
- [55] M. Stone, J. Hayward, C. Huang, Z. E. Huma, and J. Sanchez, "Mechanisms of regulation of the chemokine-receptor network," *International Journal of Molecular Sciences*, vol. 18, no. 2, p. 342, 2017.
- [56] G. Santulli, D. Lewis, A. des Georges, A. R. Marks, and J. Frank, "Ryanodine receptor structure and function in health and disease," *Subcellular Biochemistry*, vol. 87, pp. 329–352, 2018.
- [57] G. Meissner, "The structural basis of ryanodine receptor ion channel function," *The Journal of General Physiology*, vol. 149, no. 12, pp. 1065–1089, 2017.
- [58] J. K. Foskett, C. White, K. Cheung, and D. D. Mak, "Inositol trisphosphate receptor Ca<sup>2+</sup> release channels," *Physiological Reviews*, vol. 87, no. 2, pp. 593–658, 2007.
- [59] J.-P. Decuypere, G. Monaco, L. Missiaen et al., "IP<sub>3</sub> Receptors, Mitochondria, and Ca<sup>2+</sup> Signaling: Implications for Aging," *Journal of Aging Research*, vol. 2011, Article ID 920178, 20 pages, 2011.
- [60] T. Vervloessem, D. I. Yule, G. Bultynck, and J. B. Parys, "The type 2 inositol 1,4,5-trisphosphate receptor, emerging functions for an intriguing Ca<sup>2+</sup>-release channel," *Biochimica et Biophysica Acta (BBA) - Molecular Cell Research*, vol. 1853, no. 9, pp. 1992–2005, 2014.
- [61] H. Ivanova, T. Vervliet, L. Missiaen, J. B. Parys, H. De Smedt, and G. Bultynck, "Inositol 1,4,5-trisphosphate receptor-isoform diversity in cell death and survival," *Biochimica et Biophysica Acta (BBA) - Molecular Cell Research*, vol. 1843, no. 10, pp. 2164–2183, 2014.
- [62] D. L. Prole and C. W. Taylor, "Inositol 1,4,5-trisphosphate receptors and their protein partners as signalling hubs," *The Journal of Physiology*, vol. 594, no. 11, pp. 2849–2866, 2016.
- [63] R. M. Empson, P. R. Turner, R. Y. Nagaraja, P. W. Beesley, and T. Knöpfel, "Reduced expression of the Ca<sup>2+</sup> transporter protein PMCA2 slows Ca<sup>2+</sup> dynamics in mouse cerebellar Purkinje neurones and alters the precision of motor coordination," *The Journal of Physiology*, vol. 588, no. 6, pp. 907–922, 2010.
- [64] E. Carafoli and J. Krebs, *Calcium Homeostasis*, Springer Berlin Heidelberg, Berlin, Germany, 1st edition, 2000.
- [65] D. Choquette, G. Hakim, A. G. Filoteo, G. A. Plishker, J. R. Bostwick, and J. T. Penniston, "Regulation of plasma membrane Ca<sup>2+</sup> ATPases by lipids of the phosphatidylinositol cycle," *Biochemical and Biophysical Research Communications*, vol. 125, no. 3, pp. 908–915, 1984.
- [66] L. Missiaen, L. Raeymaekers, F. Wuytack, M. Vrolix, H. De Smedt, and R. Casteels, "Phospholipid-protein interactions of the plasma-membrane Ca<sup>2+</sup>-transporting ATPase. Evidence for a tissue-dependent functional difference," *Biochemical Journal*, vol. 263, no. 3, pp. 687–694, 1989.
- [67] J. T. Penniston, R. Padányi, K. Pászty, K. Varga, L. Hegedűs, and A. Enyedi, "Apart from its known function, the plasma membrane Ca<sup>2+</sup>-atpase can regulate Ca<sup>2+</sup> signaling by controlling phosphatidylinositol 4,5-bisphosphate levels," *Journal of Cell Science*, vol. 127, no. 1, pp. 72–84, 2014.
- [68] K. J. Alzayady, L. Wang, R. Chandrasekhar, L. E. Wagner, F. Van Petegem, and D. I. Yule, "Defining the stoichiometry of inositol 1,4,5-trisphosphate binding required to initiate Ca<sup>2+</sup> release," *Science Signaling*, vol. 9, no. 422, p. ra35, 2016.
- [69] X. Wu, L. Weng, J. Zhang, X. Liu, and J. Huang, "The plasma membrane calcium ATPases in calcium signaling network," *Current Protein & Peptide Science*, vol. 19, no. 8, pp. 813–822, 2018.



**Hindawi**

Submit your manuscripts at  
[www.hindawi.com](http://www.hindawi.com)

